LANGMUIR Article
Cite This: *Langmuir* XXXX, XXX, XXX−XXX
pubs.acs.org/Langmuir

Surface Nanobubbles Nucleate Liquid Boiling

Jintao Zou,[†,∥] Hongguang Zhang,[†,∥] Zhenjiang Guo,[†] Yawei Liu,[†] Jiachen Wei,[‡,§] Yan Huang,*[,†] and Xianren Zhang*[,†]

[†]State Key Laboratory of Organic−Inorganic Composites, Beijing University of Chemical Technology, Beijing 100029, China
[‡]State Key Laboratory of Nonlinear Mechanics, Institute of Mechanics, Chinese Academy of Sciences, 15 Beisihuanxi Road, Beijing 100190, China
[§]School of Engineering Science, University of Chinese Academy of Sciences, Beijing 100049, China

ABSTRACT: Surface nanobubbles have been presumed to lead to the experimental observation that liquid boiling often occurs at a much lower supersaturation than expected, yet no qualitative theory exists to explain how they participate in the process. Here, we report through a simple theoretical analysis on how the metastable nanobubbles nucleate the liquid-to-vapor transition by serving as an intermediate phase. The appearance of metastable nanobubbles inhibits the shrink of the bubble nucleus and changes bubble nucleation into a multistep process. We show three possible mechanisms for heterogeneous nucleation starting from metastable surface nanobubbles: nucleation from pinned nanobubbles, nucleation via nanobubble depinning, and nucleation through nanobubble coalescence, each predicting a significant reduction in a nucleation barrier. The occurrence of a specific nucleation pathway of bubble nucleation depends on the detailed geometry of local substrate roughness. These results give insight into how the appearance of surface nanobubbles changes the nucleation mechanisms of liquid boiling.

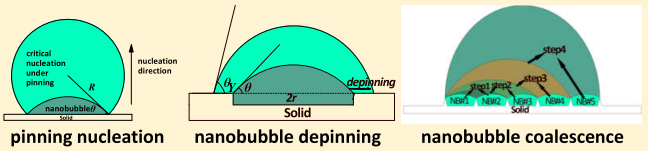

pinning nucleation nanobubble depinning nanobubble coalescence

INTRODUCTION

Within classical nucleation theory (CNT), for the occurrence of a liquid-to-vapor transition through homogeneous nucleation, a bubble nucleus is at first formed in the bulk solution. Only when the size of the nucleus exceeds a critical size after which a high energy barrier is crossed, the nucleus would grow spontaneously, leading to phase transition (Figure 1a). Different from homogeneous nucleation, which randomly occurs in the bulk solution, the heterogeneous nucleation always takes place at nucleation sites on solid surfaces or near impurities (Figure 1b). Heterogeneous nucleation usually corresponds to a lower free-energy barrier, as predicted by classical nucleation theory (CNT). Therefore, compared to homogeneous nucleation, heterogeneous nucleation is much more frequently found. Liquid boiling is one of the most common events that take place from daily life to chemical, petroleum, and power-generation industries. In spite of the significant progress made in improving our understanding of the process and correlation models working well, we are still unable to accurately predict the nucleation rate of boiling through mechanistic models.[1,2]

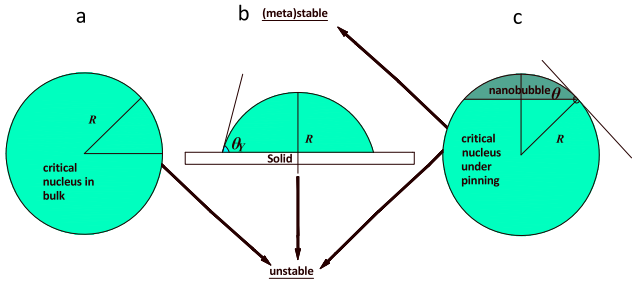

Figure 1. Relationship of the critical nucleus for (a) homogenous nucleation, (b) heterogeneous nucleation, and (c) pinning nucleation from a nanobubble. Note that the nanobubbles in (c) have the same curvature radius as that in (a) homogenous nucleation and in (b) heterogeneous nucleation.

Recent advanced surface-treatment techniques enable us to control the microstructure of substrates to remove/trap a vapor as the seed for the bubble nucleation. At the present time, the threshold of bubble nucleation obtained in many experimental studies is often much lower than that expected from classical theory. It is now widely accepted that micrometrical vapor/gas trapped in imperfections such as cavities and scratches on heated surfaces may serve as nuclei for bubbles,[3−12] and most observed nucleation in fact originates from pre-existing gas/vapor cavities. For vapor-trapping,[8−12] which works for bubble nucleation after the dissolved gas is removed, Griffith and Wallis[8] particularly developed a predictive model for the required superheat to activate vapor-trapping cavities.

Although the vapor-trapping mechanism was confirmed by numerous experimental results, there exist many cases demonstrating that gas/vapor bubble trapping in a cavity cannot be responsible for nucleation site formation. Theofanous et al.[13] found bubbles nucleated at a few tens of degrees in superheat on the surface with a mean roughness of 4 nm, for which micrometrical gas/vapor bubble trapping was not available. Bon et al.[14] also observed that the incipient superheat was low on ultrasmooth metallic surfaces. Bourdon et al.[15] studied the effect of wettability on the onset of boiling on nanometrically smooth

Received: September 27, 2018
Published: November 1, 2018

DOI: 10.1021/acs.langmuir.8b03290
Langmuir XXXX, XXX, XXX−XXX

surfaces; therefore, they speculated that surface nanobubbles may play a role on the surface even after 1 h of degassing. Qi and Klausner[16] also provided convincing evidence that the vapor-trapping mechanism was not responsible for bubble incipience. They hypothesized that nanobubbles serve as a nucleation site for heterogeneous nucleation. Nam and Ju[17] found that the onset of nucleate boiling on the nanoscopically smooth hydrophobic surface occurred at very low minimum surface superheat and assumed the existence of interfacial nanobubbles on the microcavity-free surface. Note that although several studies hypothesized that nanobubbles for heterogeneous nucleation may occur in the phase transition, no supporting data were given.

In recent years, our understanding of surface nanobubble formation and stability has been improved considerably, which inspires us to revisit the idea of whether and how nanobubbles influence the bubble nucleation. Surface nanobubbles are most frequently found on hydrophobic substrates immersed in solutions, exhibiting remarkable stability with a lifetime of hours or even days.[18−29] Their stability has been interpreted by the mechanism of contact line pinning[30−38] because of the appearance of the nanosized chemical and physical heterogeneities of substrates. Here, we propose nonlocal nucleation mechanisms with surface nanobubbles involved, i.e., nanobubble-mediated nucleation, which frequently predicts a much lower energy barrier than expected.

RESULTS AND DISCUSSION

For homogeneous nucleation (see Figure 1a), CNT gives the free-energy cost, ΔG_{homo}, for the formation of a critical nucleus of R^*

$$\Delta G_{homo} = -\Delta P(4\pi R^{*3}/3) + \gamma(4\pi R^{*2}) = 4\pi\gamma R^{*2}/3 \quad (1)$$

with γ is the vapor−liquid interface tension and ΔP the pressure difference across the interface. Equation 1 means that for the critical nucleus (the bubbles having a critical size could lead to the liquid-to-vapor transition),[39] the Laplace−Young equation works, namely, $R^* = 2\gamma/\Delta P$.

Another nucleation mechanism for the liquid-to-vapor transition is heterogeneous nucleation (see Figure 1b), through which a bubble is initiated from a solid surface. The required energy barrier for nucleating a critical nucleus, ΔG_{het}, is a function of the Young's contact angle θ_Y for the bubble on the surface (Figure 1b). Note that in this work we used the Young's contact angle of the bubble but not that of droplets to represent substrate hydrophobicity. Therefore, a smaller θ_Y represents a more hydrophobic substrate. According to CNT, ΔG_{het} is given as follows

$$\Delta G_{het}/\Delta G_{homo} = (2 - 3\cos\theta_Y + \cos^3\theta_Y)/4. \quad (2)$$

Nucleation from Pinned Nanobubbles. Then, we considered situations for which the substrate is either chemically or geometrically heterogeneous at the nanoscale, and the heterogeneities can stabilize nanobubbles at low supersaturation (normally superheat for liquid boiling).[32] We express the excess free energy for generating a pinned surface nanobubble as $\Delta G_{NB} = -V\Delta p + A\gamma$. As the contact line of the nanobubble is pinned by the substrate heterogeneity, the contributions from the solid−liquid and solid−vapor interfaces can be ignored here as they are constant. As indicated in our previous work,[40] we can identify two types of nanobubbles pinned on a base radius of r from $\frac{\partial \Delta G_{NB}}{\partial R} = 0$, one with a contact angle determined by $\sin\theta = r/R_{NB}$ (and thus $\theta < \pi/2$) and the other having a contact angle of $\pi - \theta$ (see Figure 1c for the two types of nanobubbles). Both nanobubbles have the same curvature radius R_{NB}, which is equal to that of the critical nucleus for homogeneous nucleation ($R_{NB} = R^*$).[40] This particular geometric property of nanobubbles substantially simplifies our analysis of nucleation with nanobubbles involved, as shown below.

The stability analysis demonstrated that $\frac{\partial^2 \Delta G_{NB}}{\partial R_{NB}^2} = 2\pi\gamma_{lv}\frac{(1-\cos\theta)^2}{\cos\theta}$.[40] Thus, for the smaller pinned nanobubbles with $\theta < \pi/2$, $\cos\theta > 0$ and $\frac{\partial^2 \Delta G_{NB}}{\partial R_{NB}^2} > 0$, meaning that the smaller pinned nanobubble corresponds to a local free-energy minimum and is thus thermodynamically metastable (Figure 1c). For the larger nanobubble, however, $\theta > \pi/2$, $\cos\theta < 0$, and $\frac{\partial^2 \Delta G_{NB}}{\partial R_{NB}^2} < 0$, so that the larger bubble corresponds to the pinned nanobubble that loses its stability, which would lead to the liquid-to-vapor phase transition under pinning conditions (Figure 1c). Thus, it serves as the critical nucleus for pinning nucleation.

We determined the energy change for forming the stable nanobubble with $\theta < \pi/2$ and ΔG_{NB}, and as indicated in ref 39, we have

$$\Delta G_{NB}/\Delta G_{homo} = (-V\Delta p + A\gamma)/\Delta G_{homo} = (1 - \cos^3\theta)/2 \quad (3)$$

Then, we determined the energy barrier for nucleating a liquid-to-vapor transition from the pre-existing nanobubbles with a pinning radius r (see the inset of Figure 2a). The energy barrier, ΔG_{NB}^{pin}, corresponds to the energy cost needed to expand the smaller (metastable) nanobubble to the larger (unstable) nanobubble and thus we have

$$\Delta G_{NB}^{pin}/\Delta G_{homo} = (\Delta G_{homo} - 2\Delta G_{NB})/\Delta G_{homo} = \cos^3\theta \quad (4)$$

Figure 2a shows the energy barrier for pinning nucleation ΔG_{NB}^{pin}, which decreases with the increasing pinning size (base radius). As a comparison, the figure also shows the energy change for forming a nanobubble ΔG_{NB}, which, in contrast, increases with the pinning size. Therefore, the formation of nanobubbles and their destabilization follow a different tendency, e.g., smaller nanobubbles can easily form but are difficult to destabilize for nucleation. When θ increases from 0 to $\pi/2$ ($\pi/2$ corresponds to the maximal of θ for a stable nanobubble), the nucleation barrier from a pre-existing nanobubble decreases accordingly, in agreement with Figure 2a since $\sin\theta = r/R$.[30]

The required energy barrier of nucleation from a pinned nanobubble ΔG_{NB}^{pin} is also given as a function of the contact angle of the pre-existing nanobubble, θ (see Figure 2b). As a comparison, the energy barrier $\Delta G_{het}(\theta_Y)$ for heterogeneous nucleation in the absence of surface nanobubbles is also given. The comparison indicates that the occurrence of classical heterogeneous nucleation or nonclassical pinning nucleation depends on the substrate hydrophobicity θ_Y and the contact angle of pre-existing nanobubbles θ. In detail, when the pre-existing nanobubbles have a relatively large volume, the nucleation would initially take place from the pre-existing nanobubbles, whereas if there are no pre-existing nanobubbles or the substrates are rather hydrophobic in nature, heterogeneous nucleation dominates the liquid-to-vapor transition.

DOI: 10.1021/acs.langmuir.8b03290
Langmuir XXXX, XXX, XXX−XXX

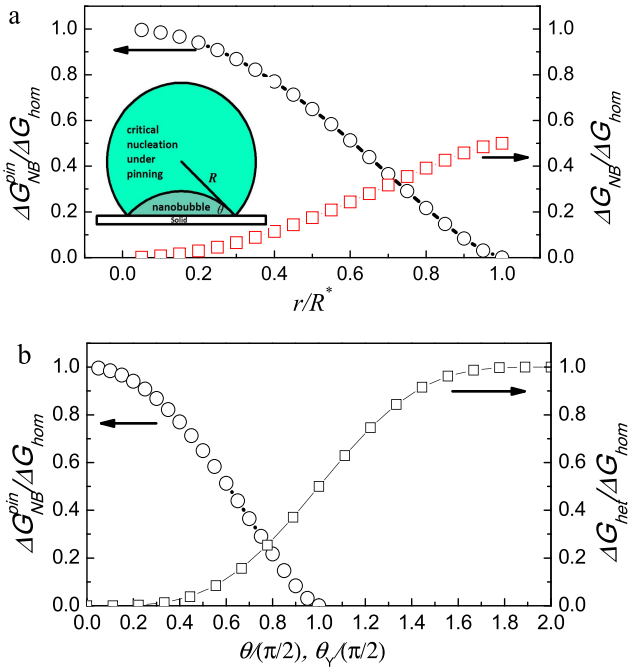

Figure 2. (a) Energy change for forming a nanobubble ΔG_{NB} and the nucleation barrier for liquid-to-vapor transition from the nanobubble ΔG_{NB}^{pin}, as a function of the base size of the nanobubble. The inset shows schematically the nucleation mechanism under pinning of the nanobubble contact line. (b) Nucleation barrier ΔG_{NB}^{pin} as a function of the contact angle for the pre-existing nanobubble, θ, and its comparison with that for the heterogeneous nucleation in the absence of nanobubble ΔG_{het} as a function of surface hydrophobicity, θ_Y.

Nucleation from Nanobubble Depinning. Different substrate microstructures show different abilities to pin the contact line of surface nanobubbles.[31] For example, concave-shaped roughness generates only the pinning force that restricts the shrink of the contact line of nanobubbles, but the expansion of the nanobubble contact line is free of constraint.[31] Therefore, pre-existing nanobubbles on pores can be easily expanded (depinned) as a starting point for depinning nucleation (see Figure 3a).

In practice, the depinning nucleation tends to occur for nanobubbles formed on the rim of a pore. In this case, nucleation from the pre-existing nanobubble would always have a small energy barrier than that from heterogeneous nucleation (Figure 3b). This is because although the nanobubble-mediated nucleation takes effect via exceeding the same critical nucleus as heterogeneous nucleation, the nanobubbles covering the substrate would certainly induce a lower nucleation barrier (Figure 3b).

Nucleation through Nanobubble Coalescence. We previously demonstrated[41] that tuning the microstructural shape of substrates can dramatically influence the dynamics of the dewetting transition. It was shown that the cone-shaped structure requires a lower barrier for the occurrence of dewetting transition than other structural topologies. Accordingly, here we propose that the neighboring nanobubbles pinned on the same cone-shaped posts may coalesce into a larger one (see Figure 4a). The step-by-step coalescence of neighboring nanobubbles would increase the nanobubble size gradually and finally reach a size of losing its stability, thus leading to liquid-to-vapor transition.

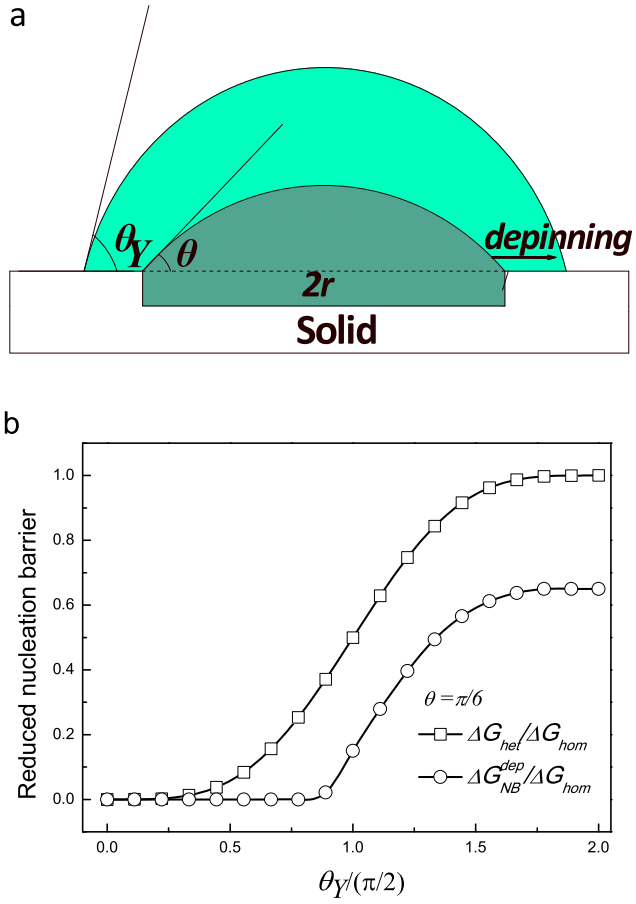

Figure 3. Panel (a) shows schematically that heterogeneous nucleation can take place on the top of a pre-existing nanobubble through contact line depinning. (b) Reduced energy barrier of heterogeneous nucleation through depinning from a pre-existing nanobubble, and its comparison with the energy barrier for the heterogeneous nucleation in the absence of the nanobubble.

For example, as shown in Figure 4a, we assumed five neighboring nanobubbles covering an area within a radius of R. (Here $r = R$ means that at the last step, the bubble becomes unstable and leads to the phase transition spontaneously.) When the left nanobubble (NB#1) pinned at a range of $R/5$ combines with its neighbor (NB#2) and reaches an intermediate nanobubble (NB#1 + 2), as indicated in step 1 in Figure 4a, we can calculate the corresponding energy cost for the intermediate state according to

$$\Delta G_{step}^{1}/\Delta G_{home} = (\Delta G_{NB}^{1+2} - (\Delta G_{NB}^{1} + \Delta G_{NB}^{2}))/\Delta G_{homo} \quad (5)$$

Thus, we obtained $\Delta G_{step}^{1}/\Delta G_{home} = 0.055$. Then, if the larger nanobubble (NB#1 + 2) formed by nanobubbles NB#1 and NB#2 grows continuously by combining its neighbor, the nanobubble NB#3, the coalescence requires energy costs of ΔG_{step}^{2} and $\Delta G_{step}^{2}/\Delta G_{home} = \frac{\Delta G_{NB}^{1+2+3} - (\Delta G_{NB}^{1+2} + \Delta G_{NB}^{3})}{\Delta G_{home}} = 0.099$. In a similar way, we can determine the following coalescence events with energy costs

$$\Delta G_{step}^{3}/\Delta G_{home} = \frac{\Delta G_{NB}^{1+2+3+4} - (\Delta G_{NB}^{1+2+3} + \Delta G_{NB}^{4})}{\Delta G_{home}}$$

$$= 0.12$$

DOI: 10.1021/acs.langmuir.8b03290
Langmuir XXXX, XXX, XXX−XXX

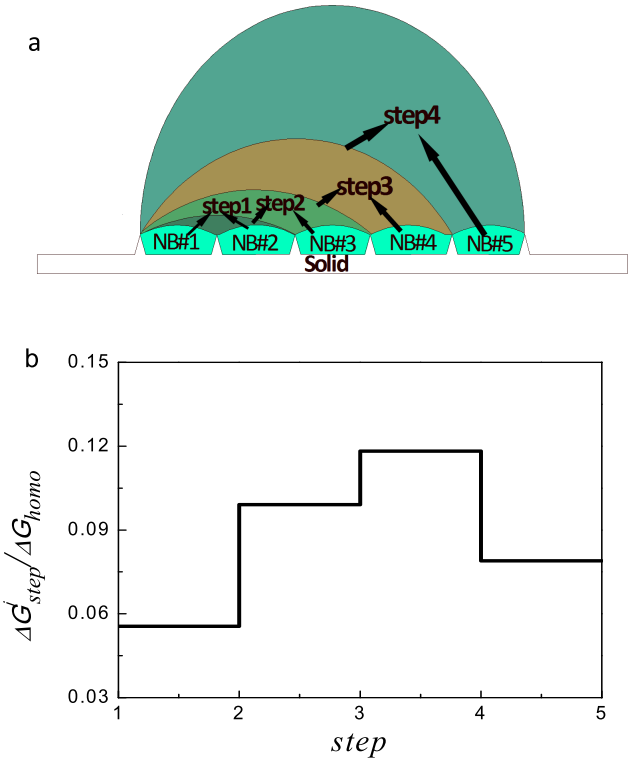

Figure 4. (a) Sketch of a nonclassical nucleation pathway with a lower energy barrier through a step-by-step coalescence of neighboring surface nanobubbles. (b) Corresponding energy cost for each event for the step-by-step coalescence of neighboring nanobubbles.

and

$$\Delta G^{4}_{\text{step}}/\Delta G_{\text{home}} = \frac{\Delta G^{1+2+3+4+5}_{\text{NB}} - (\Delta G^{1+2+3+4}_{\text{NB}} + \Delta G^{5}_{\text{NB}})}{\Delta G_{\text{home}}} = 0.079$$

The details of energy cost for each event of multiple-step nucleation mechanism through nanobubble coalescence are shown in Figure 4b. This figure clearly indicates that nanobubble coalescence can substantially reduce the nucleation barrier for the liquid-to-vapor phase transition with a multiple-step process. Therefore, we proposed that boiling nucleation may take a pathway of depinning or coalescence of neighboring nanobubbles, which effectively reduces the height of the energy barrier to be crossed, and this special nucleation mechanism can partially interpret the disagreement between experiments and CNT and could be generalized into crystallization.

Directed Nucleus Growth Due to Metastability of Surface Nanobubbles and Surface-Geometry-Determined Nucleation Pathways. In above examples of nanobubble-enhanced nucleation, metastable nanobubbles as an intermediate phase dramatically accelerate the nucleation of a phase transition between vapor and liquid. In comparison to nanobubble-free nucleation from the ideal crevice model (Figure 5a), we show above with a simple theoretical analysis that nucleation via an intermediate nanobubble state can be rather complex. The intermediate nanobubble phase could be activated in a rather low supersaturated environment. Once surface nanobubbles occur at a surface with nanosized roughness, the nucleation of the bubble becomes a stepwise process, proceeding via one or several steps that involve intermediate (and metastable) nanobubbles (Figure 5b–d). The means that the nucleation barrier for each process should decrease significantly as the intermediate phase approaches metastability (Figure 5f–h), leading to much more rapid nucleation rate. Below, we illustrate that nanobubble metastability causes the directed growth of the bubble nucleus and the occurrence of a specific nucleation pathway of bubble nucleation depends on the detailed geometry of local substrate roughness (see Figure 5).

As we demonstrated before,[31] various substrate microstructures have different abilities to pin the contact line of surface nanobubbles. In Figure 5b–d, we demonstrate the essential role of the local shape of roughness in nanobubble stability. For example, a single crevice in Figure 5c creates a pinning force that prevents the receding of the nanobubble contact line, thus inhibiting the nanobubble shrink. However, this kind of substrate geometry is unable to exert the pinning force to prevent the nanobubble contact line from advancing. As a result, the microscopic structure of the substrate roughness stabilizes the formed nanobubble in a single direction: it restricts the nanobubble shrink, while nanobubble expansion is free of constraint. This means that there exists an energy barrier for

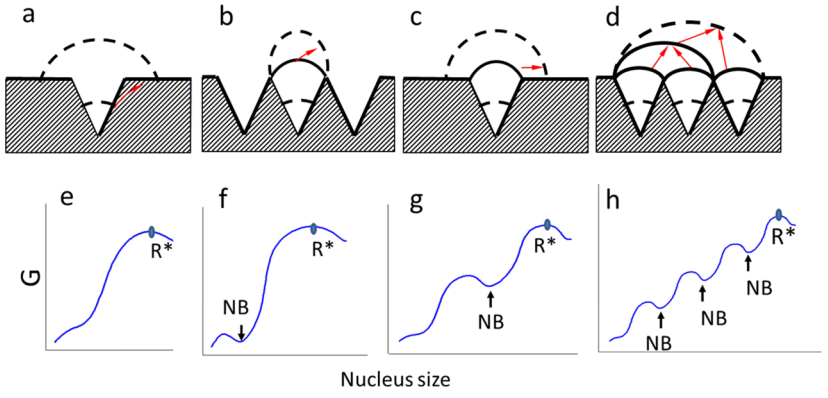

Figure 5. (a–d) Diagram showing the nucleus growing from possible ideal configurations of a vapor-trapping crevice via a pathway (a) without and (b–d) with surface nanobubbles involved: (a) traditional vapor-trapping pathway, (b) nucleation from a pinned nanobubble, (c) nucleation via nanobubble depinning, and (d) nucleation through nanobubble coalescence. In this picture, metastable surface nanobubbles are illustrated in solid lines and arrows show the direction of nucleus growth. (e–h) Corresponding energy barriers for different nucleation pathways are illustrated beneath the local structure of the crevice (a–d).

DOI: 10.1021/acs.langmuir.8b03290
Langmuir XXXX, XXX, XXX–XXX

reducing the nanobubble volume (Figure 5g), leading to the directed growth of the nucleus from the surface nanobubble. Differently, the local geometry of the substrate shown in Figure 5b provides pinning forces in two directions: they prevent the contact line from both receding and advancing. Therefore, the pinned nanobubble has to grow via a pathway of pinning transition from the smaller (metastable) nanobubble to the larger (unstable) nanobubble, sometimes requiring a higher energy barrier (Figure 5f). However, for the same local structure, if there are multiple pre-existing nanobubbles appearing near each other, they easily coalesce (Figure 5d), again leading to the directed growth of the bubble nucleus and inhibiting its shrink (Figure 5h).

CONCLUSIONS

Liquid boiling has great fundamental and practical importance, and the mechanistic models of nucleation, in contrast to the empirical model, have had limited success for predicting liquid boiling. Especially, numerous reported data suggest that bubble nucleation on surfaces with nanosized roughness may occur close to the thermodynamic saturation temperature, contradicting the prediction from the vapor-trapping mechanism of heterogeneous bubble nucleation. This apparent contradiction leads us to speculate that there exist other nucleation mechanisms with a much lower nucleation barrier. Here, we show, through a simple theoretical analysis, how surface nanobubbles, which are stabilized by nanosized surface heterogeneities, change bubble nucleation into a multistep process and promote liquid-to-vapor phase transition by inhibiting nucleus shrink. Three possible mechanisms for heterogeneous nucleation with pre-existing metastable nanobubbles are demonstrated with effectively reduced nucleation barriers: nucleation from a pinned nanobubble, nucleation via nanobubble depinning, and nucleation through nanobubble coalescence. We also illustrate that the occurrence of a specific nucleation pathway of bubble nucleation depends on the detailed geometry of local substrate roughness. These results deepen our understanding of how nanobubbles appearing on inhomogeneous substrates change the nucleation mechanisms of liquid boiling.

AUTHOR INFORMATION

Corresponding Authors

*E-mail: huangyan@mail.buct.edu.cn (Y.H.).
*E-mail: zhangxr@mail.buct.edu.cn (X.Z.).

ORCID

Jiachen Wei: 0000-0003-3802-5310
Xianren Zhang: 0000-0002-8026-9012

Author Contributions

‖J.Z. and H.Z. contributed equally to this work

Notes

The authors declare no competing financial interest.

ACKNOWLEDGMENTS

The authors thank Professor Daan Frenkel from the University of Cambridge and Professor Jure Dobnikar from the Institute of Physics, Chinese Academy of Sciences for the stimulating discussion on this study. This work is supported by the National Natural Science Foundation of China (Grant No. 91434204).

REFERENCES

(1) Caupin, F.; Herbert, E. Cavitation in water: A review. *C. R. Phys.* **2006**, *7*, 1000−1017.
(2) Dhir, V. K. Boiling heat transfer. *Annu. Rev. Fluid Mech.* **1998**, *30*, 365−401.
(3) Harvey, E. N.; Barnes, D. K.; McElroy, W. D.; Whiteley, A. H.; Pease, D. C.; Cooper, K. W. Bubble formation in animals. I. Physical factors. *J. Cell Comp. Physiol.* **1944**, *24*, 1−22.
(4) Strasberg, M. Onset of ultrasonic cavitation in tap water. *J. Acoust. Soc. Am.* **1959**, *31*, 163−176.
(5) Apfel, R. E. Role of impurities in cavitation threshold determination. *J. Acoust. Soc. Am.* **1970**, *48*, 1179−1186.
(6) Atchley, A. A.; Prosperetti, A. The crevice model of bubble nucleation. *J. Acoust. Soc. Am.* **1989**, *86*, 1065−1084.
(7) Borkent, B. M.; Gekle, S.; Prosperetti, A.; Lohse, D. Nucleation threshold and deactivation mechanisms of nanoscopic cavitation nuclei. *Phys. Fluids* **2009**, *21*, No. 102003.
(8) Griffith, P.; Wallis, J. D. The Role of Surface Conditions in Nucleate Boiling. *Chem. Eng. Prog., Symp. Ser.* **1960**, *3056*, 49−63.
(9) Sernas, V.; Hooper, F. C. The Initial Vapor Bubble Growth on a Heated Wall During Nucleation Boiling. *Int. J. Heat Mass Transfer* **1969**, *12*, 1627−1639.
(10) Preckshot, G. W.; Denny, V. E. Explorations of Surface and Cavity Properties on the Nucleation Boiling of Carbon Tetrachloride. *Can. J. Chem. Eng.* **1967**, *45*, 241−249.
(11) Rammig, R.; Weiss, R. Growth of Vapor Bubbles From Artificial Nucleation Sites. *Cryogenics* **1991**, *31*, 64−69.
(12) Kosky, P. G. Nucleation Site Instability in Nucleate Boiling. *Int. J. Heat Mass Transfer* **1968**, *11*, 929−932.
(13) Theofanous, T. G.; Tu, J. P.; Dinh, A. T.; Dinh, T. N. The Boiling Crisis Phenomenon Part I: Nucleation and Nucleate Boiling Heat Transfer. *Exp. Therm. Fluid Sci.* **2002**, *26*, 775−792.
(14) Bon, B.; Guan, C.-K.; Klausner, J. F. Heterogeneous nucleation on ultra-smooth surfaces. *Exp. Therm. Fluid Sci.* **2011**, *35*, 746−752.
(15) Bourdon, B.; Bertrand, E.; Di Marco, P.; Marengo, M.; Rioboo, R.; De Coninck, J. Wettability influence on the onset temperature of pool boiling: experimental evidence onto ultra-smooth surfaces. *Adv. Colloid Interface Sci.* **2015**, *221*, 34−40.
(16) Qi, Y.; Klausner, J. F. Comparison of nucleation site density for pool boiling and gas nucleation. *J. Heat Transfer* **2006**, *128*, 13.
(17) Nam, Y.; Ju, Y. S. Bubble nucleation on hydrophobic islands provides evidence to anomalously high contact angles of nanobubbles. *Appl. Phys. Lett.* **2008**, *93*, No. 103115.
(18) Lohse, D.; Zhang, X. Surface nanobubbles and nanodroplets. *Rev. Mod. Phys.* **2015**, *87*, 981−1035.
(19) Lou, S.-T.; Ouyang, Z.-Q.; Zhang, Y.; Li, X.-J.; Hu, J.; Li, M.-Q.; Yang, F.-J. Nanobubbles on solid surface imaged by atomic force microscopy. *J. Vac. Sci. Technol., B: Microelectron. Nanometer Struct.* **2000**, *18*, 2573.
(20) Ishida, N.; Inoue, T.; Miyahara, M.; Higashitani, K. Nano bubbles on a hydrophobic surface in water observed by tapping-mode atomic force microscopy. *Langmuir* **2000**, *16*, 6377−6380.
(21) Christenson, H. K.; Claesson, P. M. Direct measurements of the force between hydrophobic surfaces in water. *Adv. Colloid Interface Sci.* **2001**, *91*, 391−436.
(22) Attard, P. Nanobubbles and hydrophobic attraction. *Adv. Colloid Interface Sci.* **2003**, *104*, 75−91.
(23) Zhang, X. H.; Maeda, N.; Craig, V. S. Physical properties of nanobubbles on hydrophobic surfaces in water and aqueous solutions. *Langmuir* **2006**, *22*, 5025−5035.
(24) Yang, S.; Dammer, S. M.; Bremond, N.; Zandvliet, H. J.; Kooij, E. S.; Lohse, D. Characterization of nanobubbles on hydrophobic surfaces in water. *Langmuir* **2007**, *23*, 7072−7077.
(25) Zhang, X. H.; Quinn, A.; Ducker, W. A. Nanobubbles at the interface between water and a hydrophobic solid. *Langmuir* **2008**, *24*, 4756−4764.
(26) Wang, X.; Zhao, B.; Ma, W.; Wang, Y.; Gao, X.; Tai, R.; Zhou, X.; Zhang, L. Interfacial Nanobubbles on Atomically Flat Substrates with Different Hydrophobicities. *ChemPhysChem* **2015**, *16*, 1003−1007.

DOI: 10.1021/acs.langmuir.8b03290
Langmuir XXXX, XXX, XXX−XXX

(27) Hampton, M. A.; Nguyen, A. V. Nanobubbles and the nanobubble bridging capillary force. *Adv. Colloid Interface Sci.* **2010**, *154*, 30−55.
(28) Walczyk, W.; Schönherr, H. Closer Look at the Effect of AFM Imaging Conditions on the Apparent Dimensions of Surface Nanobubbles. *Langmuir* **2013**, *29*, 620−632.
(29) Craig, V. S. J. Very small bubbles at surfaces—the nanobubble puzzle. *Soft Matter* **2011**, *7*, 40−48.
(30) Liu, Y.; Zhang, X. Nanobubble stability induced by contact line pinning. *J. Chem. Phys.* **2013**, *138*, No. 014706.
(31) Liu, Y.; Wang, J.; Zhang, X.; Wang, W. Contact line pinning and the relationship between nanobubbles and substrates. *J. Chem. Phys.* **2014**, *140*, No. 054705.
(32) Liu, Y.; Zhang, X. A unified mechanism for the stability of surface nanobubbles: Contact line pinning and supersaturation. *J. Chem. Phys.* **2014**, *141*, No. 134702.
(33) Weijs, J. H.; Lohse, D. Why surface nanobubbles live for hours. *Phys. Rev. Lett.* **2013**, *110*, No. 054501.
(34) Lohse, D.; Zhang, X. Pinning and gas oversaturation imply stable single surface nanobubbles. *Phys. Rev. E* **2015**, *91*, No. 031003.
(35) Zhang, X.; Chan, D. Y. C.; Wang, D.; Maeda, N. Stability of interfacial nanobubbles. *Langmuir* **2013**, *29*, 1017−1023.
(36) Zhang, X.; Lhuissier, H.; Sun, C.; Lohse, D. Surface nanobubbles nucleate microdroplets. *Phys. Rev. Lett.* **2014**, *112*, No. 144503.
(37) Teshima, H.; Nishiyama, T.; Takahashi, K. Nanoscale pinning effect evaluated from deformed nanobubbles. *J. Chem. Phys.* **2017**, *146*, No. 014708.
(38) Tan, B. H.; An, H.; Ohl, C.-D. Resolving the Pinning Force of Nanobubbles with Optical Microscopy. *Phys. Rev. Lett.* **2017**, *118*, No. 054501.
(39) Menzl, G.; Gonzalez, M. A.; Geiger, P.; Caupin, F.; Abascal, J. L. F.; Valeriani, C.; Dellago, C. Molecular mechanism for cavitation in water under tension. *Proc. Natl. Acad. Sci. U.S.A.* **2016**, *113*, 13582−13587.
(40) Xiao, Q.; Liu, Y.; Guo, Z.; Liu, Z.; Frenkel, D.; Dobnik, J.; Zhang, X. What experiments on pinned nanobubbles can tell about the critical nucleus for bubble nucleation. *Eur. Phys. J. E* **2017**, *40*, 114.
(41) Zhang, B.; Chen, X.; Dobnikar, J.; Wang, Z.; Zhang, X. Spontaneous Wenzel to Cassie dewetting transition on structured surfaces. *Phys. Rev. Fluids* **2016**, *1*, No. 073904.

DOI: 10.1021/acs.langmuir.8b03290
Langmuir XXXX, XXX, XXX−XXX